A possible regulatory role for the metal-binding domain of CadA, the *Listeria monocytogenes* Cd^{2+}-ATPase

Nathalie Bal, Elisabeth Mintz, Florent Guillain, Patrice Catty*

Commissariat à l'Energie Atomique, Département de Biologie Moléculaire et Structurale, Laboratoire de Biophysique Moléculaire et Cellulaire, UMR CEA-CNRS-UJF 5090, 17 rue des Martyrs, 38054 Grenoble Cedex 09, France

Received 27 July 2001; revised 11 September 2001; accepted 12 September 2001

First published online 26 September 2001

Edited by Ulf-Ingo Flügge

Abstract Using the baculovirus/Sf9 expression system, we produced CadA and ΔMBD, a metal-binding domain, truncated CadA. Both proteins had the expected properties of P-type ATPases: ATP-induced Cd^{2+} accumulation, Cd^{2+}-sensitive ATP and Pi phosphorylation and ATPase activity. ΔMBD displayed lower initial transport velocity as well as lower maximal ATPase activity than CadA. MBD truncation flattened the Cd^{2+} dependence of the ATPase activity and increased apparent Cd^{2+} affinity, suggesting a positive cooperativity between MBD and membranous transport sites. We propose that occupancy of MBD by Cd^{2+} modulates CadA activity.

Key words: Cadmium; Metal-binding domain; P-type ATPase; CadA

1. Introduction

P-type ATPases are ubiquitously distributed membrane proteins that actively transport a variety of ions across biological membranes. Among them, P1-ATPases have been shown to be involved in copper homeostasis [1] and in cadmium, lead and zinc resistance [2].

P1-ATPases have consensus sequences of P-type ATPases and the same core region consisting of four transmembrane helices and two cytoplasmic domains, the largest one containing the catalytic site and a highly conserved aspartate residue. P1-ATPases differ from the other P-ATPases by their topology, which is predicted to display a large amino-terminal domain containing two additional transmembrane helices and one to six cytoplasmic metal-binding domains (MBD) (see [3] for P-ATPase classification).

The P1-ATPase MBD is a 60–70 amino acid sequence first discovered in MerP (mercury-binding periplasmic protein) and MerA (mercuric reductase) and later in copper chaperones [4,5]. All the MBDs found so far contain one CxxC sequence reported to coordinate directly the metal and display the same βαββαβ secondary structure. Three-dimensional structures obtained from either X-ray diffraction or nuclear magnetic resonance have shown that regardless of the bound metal, their carbon backbones were almost superimposable [6,7]. These structural data, as well as ion-binding experiments with isolated MBDs [8–10], suggest that MBDs are not the selectivity filter of P1-ATPases.

A number of studies have looked in vivo for a role of the MBD in the physiological function of P1-ATPases. Complementation studies in *Saccharomyces cerevisiae* using the human copper ATPases ATP7A or ATP7B have shown that replacement of cysteine by serine in the six CxxC motifs or truncation of all MBDs prevented any restoration of the wild-type phenotype of a strain lacking Ccc2p, the yeast copper ATPase [11–14]. Partial deletion and mutations have also demonstrated that the sixth MBD was sufficient for ATP7B to replace Ccc2p functionally [12,14], whereas this was not the case for ATP7A [11]. In situ immunolocalization studies have shown that C to S substitutions in the six CxxC motifs impaired the physiological copper-induced relocalization of ATP7A from the *trans*-Golgi to the plasma membrane, but that either one of the fifth or sixth MBD was sufficient for such a relocalization [15]. Recent in vitro studies of a mutated ATP7A with six SxxS motifs [16,13] and of an MBD-truncated ZntA, the *Escherichia coli* Zn^{2+}-ATPase [17], have demonstrated that functional MBDs were not an absolute requirement for the ATPases to work.

In this paper, we have studied the effects of MBD truncation on the enzymatic activity of CadA, the determinant of *Listeria monocytogenes* cadmium resistance [18,19]. CadA is a 711 amino acid P1-ATPase which possesses one MBD containing one CTNC sequence and has 82% homology with the 727 amino acid Cd^{2+}-ATPase from *Staphylococcus aureus* [20] and 55% homology with the *E. coli* ZntA.

We have produced enough CadA in the Sf9/baculovirus system to be detectable by standard Coomassie blue-stained gels from SDS–PAGE. ATPase activity, Cd^{2+} accumulation, and phosphorylation demonstrated that truncated CadA was still active. However, it displayed a lower overall catalytic rate and a higher apparent affinity for cadmium.

2. Materials and methods

2.1. Wild-type and mutated forms of CadA

The 2.7 kb *Hin*dIII/*Eco*RI fragment from the pMa39 plasmid containing CadA (gift from P. Cossart, Pasteur Institute, Paris, France) was subcloned into the pSP72 plasmid (Promega, Charbonnières, France). The CadA gene was then mutated to generate the *Sst*I and *Bst*BI restriction sites (pSPCad5 plasmid), further used for subcloning into the pFastBac1 baculovirus/Sf9 expression vector. The pSPCad5 plasmid was used as a template to produce the D398A mutant and the N-terminal truncated protein. For their immunodetection, the three forms of CadA were modified by insertion of a C-terminal hemagglutinin (HA) epitope.

*Corresponding author. Fax: (33)-4-38 78 54 87.
E-mail address: catty@dsvgre.cea.fr (P. Catty).

PII: S0014-5793(01)02927-1

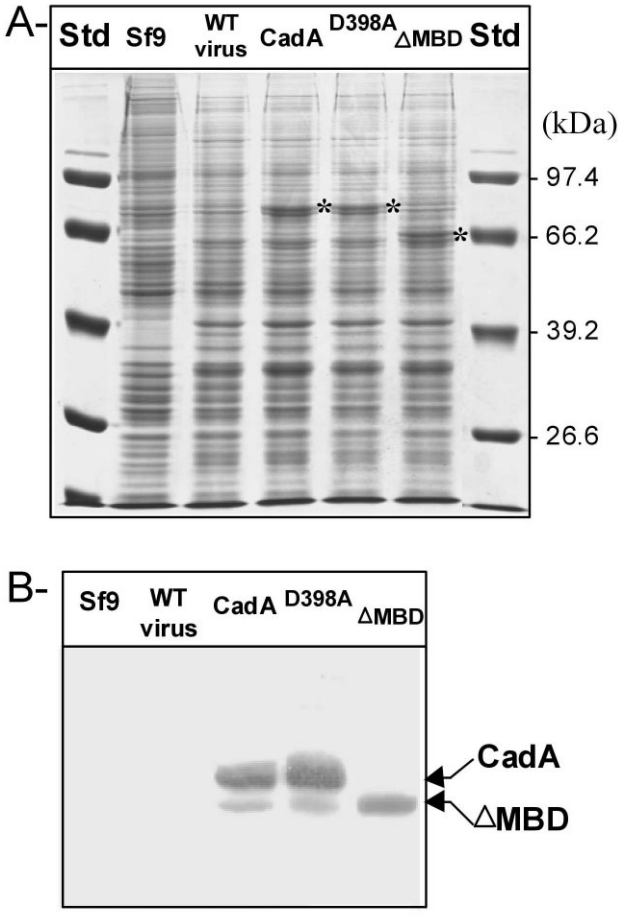

Fig. 1. Expression in Sf9 cells. Coomassie blue-stained gels of SDS–PAGE (A) and HA-tagged protein immunodetection (B) of 50 μg of methanol/chloroform-precipitated P100 fractions from non-infected cells (Sf9), cells infected with the wild-type virus (WT virus) and cells infected with a virus containing CadA, D398A or ΔMBD (indicated by black stars).

2.2. Protein preparation

The three forms of CadA were produced using the BAC-TO-BAC™ baculovirus expression system (Life Technologies, Cergy Pontoise, France). After a 3 day culture at 27°C, 100 ml of cells (4×10^6 cells/ml) were harvested by centrifugation (10 min, $500\times g$, 4°C). The pellet was resuspended in 18 ml of 10 mM MOPS–Tris (pH 7), 10 μg/ml RNase, 20 μg/ml DNase I and EDTA-free antiproteases (Roche Molecular Biochemicals, Meylan, France). Cells were lysed by potterization and the homogenate was complemented to reach 10 mM MOPS–Tris (pH 7), 80 mM KCl, 0.2 mM $MgCl_2$, 300 mM sucrose. The sample was centrifuged (1 h, $100\,000\times g$, 4°C) and the P100 pellet corresponding to a total membrane fraction was resuspended in 2 ml of 50 mM MOPS–Tris (pH 7), 100 mM KCl, 1 mM $MgCl_2$, 300 mM sucrose. The P100 protein concentration was 40–60 mg/ml. Aliquots were rapidly frozen in liquid nitrogen and stored at −80°C.

2.3. Protein detection

Protein concentration was determined using the DC protein assay (Bio-Rad, Hercules, CA, USA). Protein expression was assessed by SDS–PAGE and by immunodetection. Anti-HA-peroxidase monoclonal antibody (3F10) was from Roche Molecular Biochemicals. Protein was detected using the BM chemiluminescence Western blotting kit (Roche Molecular Biochemicals). Protein was quantitated by densitometric analysis of the Coomassie blue-stained polyacrylamide gel (Scion Image program, http://www.scioncorp.com).

2.4. Protein activity measurements

ATPase activity was measured at 28°C, by following NADH absorbance changes, using a coupled enzyme assay as described in [21]. Accumulation of $^{109}Cd^{2+}$ (Amersham Pharmacia Biotech, Saclay, France) was performed as described in [21]. Phosphorylations from ATP and from inorganic phosphate (Pi) were performed as described in [22]. The acidic gels [23] were exposed to Phosphor Screen and analyzed on a PhosphorImager (Molecular Dynamics Amersham Pharmacia Biotech). The gels were later stained with Coomassie blue in order to check the amount of loaded protein and the size of the phosphorylated bands.

3. Results

Three forms of CadA were studied: CadA, the wild-type protein, D398A, a non-phosphorylatable protein modified in the DKTGT sequence, and ΔMBD, the MBD-truncated protein constructed by removal of the first 84 amino acids and replacement of the original I85 by an M.

3.1. Production of the wild-type and mutated proteins (Fig. 1)

As shown by SDS–PAGE analysis, the baculovirus/Sf9 expression system produced significant amounts of the three forms of CadA (Fig. 1A). For comparison, the first two lanes show protein profiles of P100 fractions from non-infected Sf9 cells and from Sf9 cells infected with the wild-type virus. The next three lanes, which correspond to P100 fractions from Sf9 cells infected with recombinant viruses, displayed additional bands of expected molecular weights, 77 kDa for CadA and D398A and 68 kDa for ΔMBD. Western blot analysis of the HA-tagged variants showed that whereas ΔMBD appeared intact in the P100 fractions, CadA and D398A were slightly degraded (Fig. 1B). The size of the degradation product suggests a sensitivity of the amino-terminal region of CadA to endogenous proteases.

3.2. Enzymatic characterization of ΔMBD

Taking the Ca^{2+}-ATPase SERCA1a as model [24], the ΔMBD cycle can be described as shown in Scheme 1, which indicates how transport events (steps 1 and 3) and chemical events (steps 2 and 4) are interlinked and where n denotes the unknown number of membranous transport sites. The presence or absence of Cd^{2+} at these sites alters the chemical specificity of ATPase for phosphorylation. Cd_nE reacts with ATP in the forward direction (step 2), whereas E reacts with Pi in the backward direction (step 4). The chemical state of ATPase, in turn, determines the affinity and orientation of the transport sites. Cytoplasmic Cd^{2+} ions bind or dissociate from high-affinity sites of E (step 1), whereas extracytoplasmic Cd^{2+} ions bind or dissociate from low-affinity sites of E-P

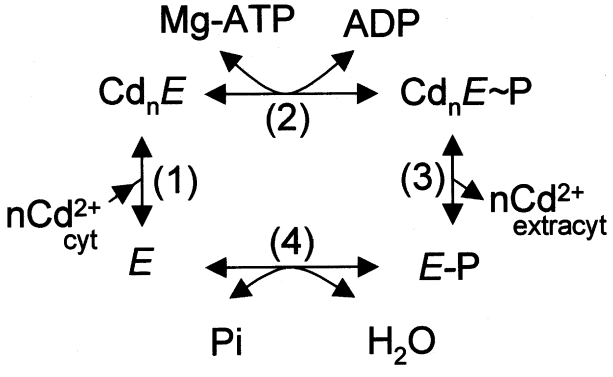

Scheme 1.

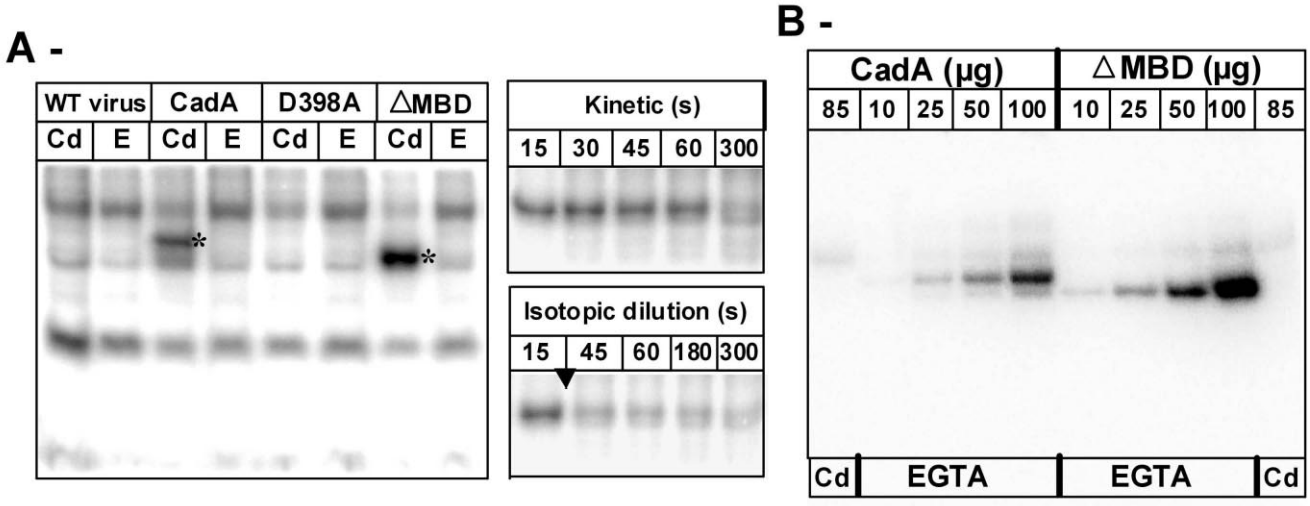

Fig. 2. Cadmium-regulated phosphorylations from ATP and inorganic phosphate. A: Phosphorylation from ATP. P100 fractions (70 μg) were phosphorylated for 15 s at 0°C in 100 μl of 30 mM MOPS–Tris (pH 7), 60 mM KCl, 1 mM $MgCl_2$, 180 mM sucrose, 50 μM thapsigargin, supplemented with either 100 μM $CdCl_2$ or 500 μM EGTA (E). The reaction was initiated by adding 1 μM [γ-^{32}P]ATP. Stars indicate the phosphorylated forms of CadA and ΔMBD. Kinetic and isotopic dilution experiments with phosphorylated ΔMBD. In the kinetic experiment, the reaction lasted 5 min and samples were acid-quenched at the indicated times. In the isotopic dilution experiment, the first sample was quenched after 15 s. ATP concentration was then increased to 10 μM by addition of cold ATP, and samples were quenched at the indicated times. B: Phosphorylation from Pi of different amounts (10–100 μg, as indicated) of P100 fractions containing CadA and ΔMBD was carried out at 25°C in 100 μl of 50 mM MES–Tris (pH 6), 10 mM $MgCl_2$, 50 μM thapsigargin, 20% (v/v) Me_2SO supplemented with either 100 μM $CdCl_2$ or 500 μM EGTA. The reaction was initiated by adding 100 μM ^{32}Pi.

(step 3). In wild-type CadA, the transport process is assumed to be the same, except for an additional role for MBD.

Assuming, as for any P-ATPase, that the phosphoenzymes are acid-stable, CadA and ΔMBD were compared for their ability to be phosphorylated from [γ-^{32}P]ATP or ^{32}Pi (Fig. 2). In panel A, which shows ATP phosphorylation, two additional labellings were detected in the P100 fractions containing CadA or ΔMBD. These labellings were only observed in the presence of Cd^{2+}, their molecular weights were in agreement with the expected values of the two proteins, and they were absent in P100 fractions from non-expressing Sf9 cells or cells expressing D398A. Hence, they were attributed to Cd^{2+}-dependent phosphoenzyme formation from ATP, suggesting that Cd^{2+} binding to the transport site does not require MBD. As expected from Scheme 1, the ΔMBD phosphoenzyme obtained from ATP was found to be transient, as illustrated by a 'kinetic' experiment where ΔMBD labelling progressively decreased due to ATP depletion, or by an 'isotopic dilution' experiment where ΔMBD labelling decreased upon [γ-^{32}P]ATP dilution.

CadA and ΔMBD were next phosphorylated from Pi in the presence of EGTA (Fig. 2B). Inhibition of this reaction by Cd^{2+} confirmed that the Cd^{2+} transport site was still functional and that Cd^{2+} binding does not require MBD.

Direct evidence that the Cd^{2+} translocation pathway was preserved in ΔMBD came from experiments depicted in Fig. 3A which showed that ΔMBD as well as CadA were able to accumulate $^{109}Cd^{2+}$ into vesicles in the presence of ATP. The major difference was in the initial velocities: 9 and 3 nmol/min/mg for CadA and ΔMBD, respectively.

Finally, ATPase activity was measured to evaluate the apparent affinity of CadA and ΔMBD for Cd^{2+}. Fig. 3B shows that both CadA and ΔMBD activities were stimulated by increasing Cd^{2+} concentrations, confirming that MBD was not essential for CadA activity in vitro. As expected, D398A displayed no Cd^{2+}-stimulated ATPase activity but rather an inhibition at high Cd^{2+} concentrations which is likely due to competition between Mg-ATP and Cd-ATP [25] in endogenous Sf9 ATPase activities. This phenomenon, together with back-inhibition (Scheme 1, step 3), would explain the observed inhibition of ΔMBD and CadA ATPase activities. Major effects of MBD truncation were found on the apparent affinity for Cd^{2+} which was shifted from 10 to 3 μM and on the shape of the Cd^{2+}-induced stimulation. The efficient concentration range was twice as broad for ΔMBD as for CadA.

4. Discussion

We have compared the enzymatic properties of CadA and ΔMBD. ΔMBD displayed the common properties of P-ATPases: active transport (Fig. 3A), Cd^{2+}-dependent ATPase activity (Fig. 3B), and ATP and Pi phosphorylations (Fig. 2), in agreement with the transport cycle (Scheme 1).

As estimated from Pi phosphoenzyme levels (Fig. 2B), taken as an indicator of ATPase functionality, ΔMBD concentration was twice that of CadA. Therefore, ΔMBD exhibited a lower maximal ATPase activity as observed with ZntA [17] and a lower initial $^{109}Cd^{2+}$ transport velocity than CadA.

ATPase activity (Fig. 3B) showed that the ΔMBD apparent affinity for Cd^{2+} is three-fold higher than that of CadA. This apparent affinity increase cannot be explained by significant changes in free Cd^{2+} concentrations that would result from different metal-binding capacities of the membranes containing either CadA or ΔMBD. As estimated from the gel (Fig. 1A), CadA or ΔMBD does not account for more than 2% of the total protein in P100 fractions. Therefore, their concentrations in ATPase assays did not exceed 0.1 μM, a concentration too low to modify significantly Cd^{2+} concentration in the range where the difference in apparent affinity is observed.

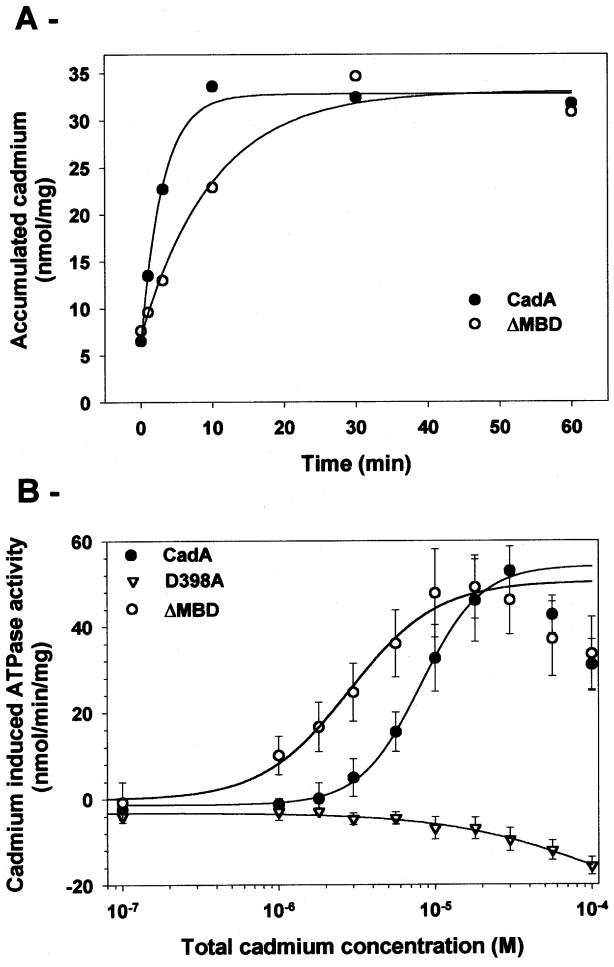

Fig. 3. Cd^{2+} accumulation and Cd^{2+}-dependent ATPase activities. A: Cd^{2+} accumulation by P100 fractions (0.2–0.3 mg/ml) was measured by a filtration method (Millipore HA 0.45 filter) in 50 mM MOPS–Tris (pH 7), 100 mM KCl, 5 mM $MgCl_2$, 20 μM thapsigargin, 10 μM $^{109}Cd^{2+}$ and 10 mM Pi, as Cd^{2+} precipitating agent. The buffer also contained 1 mM [^{3}H]glucose to evaluate the filter wet volume. The reaction was started by addition of 2 mM ATP. Activities are normalized to 1 mg of total membrane protein. B: ATPase activities of P100 fractions (0.3–0.8 mg/ml) were measured in 50 mM MOPS–Tris (pH 7), 100 mM KCl, 5 mM $MgCl_2$, 300 mM sucrose. The reaction was initiated, in the absence of Cd^{2+}, by addition of 2 mM ATP and this basal activity was subtracted from the Cd^{2+}-dependent activities. Activities are normalized to 1 mg of total membrane protein. Values are means of at least five independent experiments.

Under similar conditions, a decrease in the apparent affinity for copper was observed with the human Menkes ATPase containing six SxxS motifs [13] and limited changes in the apparent affinity for Pb^{2+}, Cd^{2+}, Zn^{2+} were observed upon truncation of ZntA [17]. Interestingly, the truncated ZntA displayed a three- to five-fold higher apparent affinity for these ions in the presence of thiolates.

The most striking effect of MBD removal was to flatten the Cd^{2+}-induced stimulation of CadA ATPase activity (Fig. 3B). Recalling that the truncation removed all the predicted cytoplasmic N-terminal amino acids, and referring to the Ca^{2+}-ATPase 3D structure [26], the ΔMBD Cd^{2+}-binding sites can only be located in the membrane. Thus, ΔMBD ATPase activity dependence upon Cd^{2+} is supposed to reflect the apparent affinity of the membranous transport sites for Cd^{2+}. Therefore, the sharper shape together with the lower apparent affinity of the CadA response to Cd^{2+} suggest a positive cooperative interaction between MBD and the membranous transport sites, the latter having a higher apparent affinity for Cd^{2+} than MBD. Further investigations are required to evaluate the stoichiometry of Cd^{2+} binding to CadA or ΔMBD and thus the number of transport sites.

Our results show that ΔMBD is constitutively active and comparison with the CadA data suggests a regulatory role for the MBD. The apo-MBD may inhibit Cd^{2+} transport by preventing Cd^{2+} binding at the membranous transport sites. The holo-MBD would allow Cd^{2+} binding at the transport sites and therefore activation of CadA. Such an activation of metal efflux could participate in bacterial resistance to toxic metals as well as in the physiological homeostasis of metals such as zinc or copper. For bacterial cadmium resistance, MBD could act as a Cd^{2+} sensor downstream of CadC regulation, which occurs at Cd^{2+} concentrations lower than 0.1 μM [27].

References

[1] Mercer, J.F.B. (2001) Trends Mol. Med. 7, 64–69.
[2] Nies, D.H. (1999) Appl. Microbiol. Biotechnol. 51, 730–750.
[3] Lutsenko, S. and Kaplan, J.H. (1995) Biochemistry 34, 15607–15613.
[4] Miller, S.M. (1999) Essays Biochem. 34, 17–30.
[5] Arnesano, F., Banci, L., Bertini, I., Huffman, D.L. and O'Halloran, V. (2001) Biochemistry 40, 1528–1539.
[6] Gitschier, J., Moffat, B., Reilly, D., Wood, W.I. and Fairbrother, W.J. (1998) Nature Struct. Biol. 5, 47–54.
[7] Banci, L., Bertini, I., Ciofi-Baffoni, S., Huffman, D.L. and O'Halloran, T.V. (2001) J. Biol. Chem. 276, 8415–8426.
[8] Cobine, P.A., George, G.N., Winzor, D.J., Harrison, M.D., Mogahaddas, S. and Dameron, C.T. (2000) Biochemistry 39, 6857–6863.
[9] Jensen, P.Y., Bonander, N., Moller, L.B. and Farver, O. (1999) Biochim. Biophys. Acta 1434, 103–113.
[10] DiDonato, M., Narindrasorasak, S., Forbes, J.R., Cox, D.W. and Sarkar, B. (1997) J. Biol. Chem. 272, 33279–33282.
[11] Payne, A.S. and Gitlin, J.D. (1998) J. Biol. Chem. 273, 3765–3770.
[12] Forbes, J.R., Hsi, G. and Cox, D.W. (1999) J. Biol. Chem. 274, 12408–12413.
[13] Voskoboinik, I., Mar, J., Strausak, D. and Camakaris, J. (2001) J. Biol. Chem. 2766, 28620–28627.
[14] Iida, M., Terada, K., Sambongi, Y., Wakabayashi, T., Miura, N., Koyama, K., Futai, M. and Sugiyama, T. (1998) FEBS Lett. 428, 281–285.
[15] Strausak, D., La Fontaine, S., Hill, J., Firth, S.D., Lockhart, P.J. and Mercer, J.F. (1999) J. Biol. Chem. 274, 11170–11177.
[16] Voskoboinik, I., Strausak, D., Greenough, M., Brooks, H., Petris, M., Smith, S., Mercer, J.F. and Camakaris, J. (1999) J. Biol. Chem. 274, 22008–22012.
[17] Mitra, B. and Sharma, R. (2001) Biochemistry 40, 7694–7699.
[18] Lebrun, M., Audurier, A. and Cossart, P. (1994) J. Bacteriol. 176, 3049–3061.
[19] Lebrun, M., Audurier, A. and Cossart, P. (1994) J. Bacteriol. 176, 3040–3048.
[20] Nucifora, G., Chu, L., Misra, T.K. and Silver, S. (1989) Proc. Natl. Acad. Sci. USA 86, 3544–3548.
[21] Miras, R., Cuillel, M., Catty, P., Guillain, F. and Mintz, E. (2001) Proteic Express. Purif. 22, 299–306.
[22] Andersen, J.P., Vilsen, B., Leberer, E. and MacLennan, D.H. (1989) J. Biol. Chem. 264, 21018–21023.
[23] Weber, K. and Osborn, M. (1969) J. Biol. Chem. 244, 4406–4412.
[24] Jencks, W.P. (1989) J. Biol. Chem. 264, 18855–18858.
[25] Toledo-Maciel, A., Goncalves-Gomes, S., de Gouveia Castex, M. and Vieyra, A. (1998) Biochemistry 37, 15261–15265.
[26] Toyoshima, C., Nakasako, M., Nomura, H. and Ogawa, H. (2000) Nature 405, 647–655.
[27] Busenlehner, L.S., Cosper, N.J., Scott, R.A., Rosen, B.P., Wong, M.D. and Giedroc, D.P. (2001) Biochemistry 40, 4426–4436.